

## Chapter 5

# PQ Compensation Using DSTATCOM

### Introduction

The extensive use of power electronic equipment in MG based distribution system results in many power quality issues. The reactive component of current is raised from the MG supply due to the nonlinear loads. Unbalanced currents and excessive neutral currents flow if the system is of three-phase. To mitigate all these current quality issues, a state-of-the-art controller like distributed static compensator (DSTATCOM) is utilized. This shunt compensator, DSTATCOM is enhanced to shunt active power filter (Shunt APF) to compensate harmonic currents and neutral currents. The compensator is designed with different control techniques such as IVTG and 3-phase p-q theory for shunt APF and analyzed for balanced loads. Further, a modified 1-phase p-q theory based control technique is proposed to improve its performance in providing current harmonic compensation during nonlinear loads with proper DC link control. This chapter investigates the control techniques applied to enhanced DSTATCOM in mitigating the current quality problems.

## 5.1 DSTATCOM in MG Distribution Systems

The CPDs, namely, DSTATCOMs, DVRs are used to mitigate various PQ problems. Out of these, voltage quality issues in MG are handled by the series APF (enhanced DVR) as discussed in the previous chapter. Similarly, DSTATCOMs will be used for mitigating the current-based power quality problems in MG. The problem of unbalanced currents due to raising in neutral or circulating currents is observed in three-phase, four-wire systems mainly due to unbalanced nonlinear loads in MG. In addition to unbalanced currents, harmonics in source currents are produced when the MG is connected to nonlinear loads. In order to deal with the problems of current harmonics, DSTATCOM is further modified as Shunt APF.

### 5.1.1 State of the Art on DSTATCOM and Shunt APF

Most of the domestic appliances (loads) behave as nonlinear loads and cause power quality problems. The traditional capacitors and SVC based TCRs and TSCs had been used to solve these problems. The classical devices used for providing PQ improvement suffer from fixed (tuned) frequencies and could not function satisfactorily under changing system configurations and /or variable (nonlinear) load conditions. In this regard, DSTATCOM technology provides compensation to neutral current, thereby achieving balance in microgrids. The DSTATCOM provides compensation at the load end which is effective in improving the performance of the system. Additionally, to mitigate current harmonics, DSTATCOM is enhanced with filtering feature and is modified as shunt APF. The investigation of DSTATCOM performance is examined when it is incorporated in an MG. Adjustable speed drives (ASD) with solid state control draw more amount of power, hence in the design of many electrical loads, APFs have been incorporated. Instantaneous reactive power theory (IRPT), synchronous reference frame (d-q) theory, synchronous detection method, notch filter method are few control techniques used for controlling shunt APFs in conventional distribution systems. The single-phase p-q theory for the purpose of active power filtering was proposed to mitigate current harmonics in the conventional distribution system in [161]. Further extraction of fundamental and/or harmonic

components present in the nonlinear currents using advanced artificial neural networks technique for shunt APF was presented in [113]. A three-phase four wire (3P4W) shunt active power filter (APF) based on H- bridge topology was presented for mitigating harmonics at load end in [162]. Mitigating current harmonics under distorted supply condition by shunt APF was discussed in [114]. A shunt APF with hysteresis current control was proposed in [115, 163]. Application of customized power devices in a DG system to enhance the power quality of main grid was presented in [116]. A single-phase active power filter in a distorted power system environment was used to improve harmonic suppression efficiency with self-tuning filter algorithm [117]. Multiple and parallel APF units were proposed to reduce the circulating currents thus enhancing the system capacity and provide operational flexibility [118]. Application of shunt APF in MG for mitigating current quality issues is yet to be investigated. MGs are always associated with power electronic interfacing which in turn demand harmonic and reactive power compensation. The realization of multitasking devices poses a new trend to handle all these power quality problems simultaneously. Shunt APFs can operate in this direction, operates at the installed point and need not consider the entire system PQ condition. In addition, they optimize the performance of the system by providing multi-tasking ( harmonic compensation, neutral compensation etc) in MGs. In the MG literature, the application of APFs in providing power quality compensation was mainly discussed for DG connected main grid [164, 165]. However, in all the situations, shunt APF is supported by MG where the function of MG is limited to support the DC link of the voltage source converter of shunt APF. The present chapter considers the condition of an MG (i.e. in islanded mode) which is operating separately from main grid and acts as a mini power system. In such case, there is no reference for frequency or voltage and the MG has to maintain its power balance independently without any support from the main grid. In this condition, it is very difficult to meet compensation requirements due to tightly coupled generation and distribution that further necessitates a compensating device to handle these issues. Hence, the shunt APF with its self-supporting DC link is utilized in microgrid distribution environment to handle the concerned power quality issues. The major issues such as VAR compensation, reduction of current harmonics and circulating current compensation of microgrids along with

DC link control are considered as key objectives in this chapter. The studies require modeling of DSTATCOM which is described in the following section.

## 5.2 Distribution STATCOM

In this section, the operation of DSTATCOM for power quality compensation is discussed. The block diagram of a DSTATCOM is shown in Figure. 5.1. The STATCOM consists of a voltage-

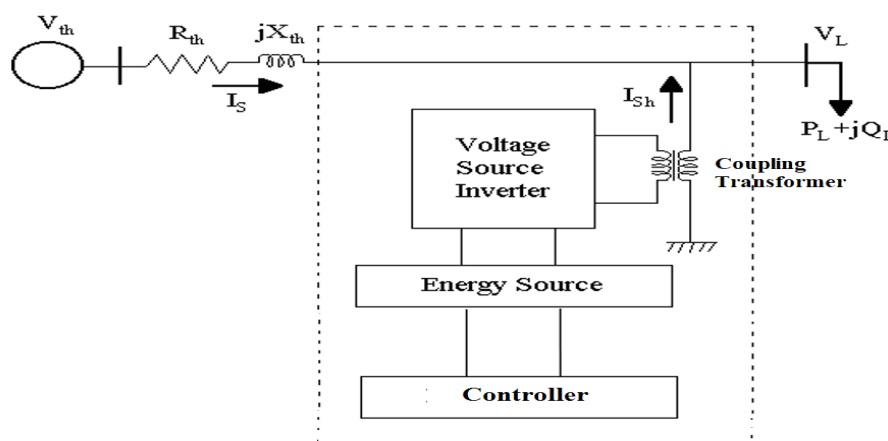


FIGURE 5.1: Block diagram of DSTATCOM

sourced inverter, a controller, an interfacing inductor or coupling transformer with neutral and a DC capacitor acting as energy storage. The STATCOM is a shunt connected FACTS device and due to its wide range of applications towards distribution system, it is turned into one of the CPDs and is named as distribution STATCOM i.e, DSTATCOM. The system reactive power is injected/absorbed by DSTATCOM and thus the voltage is regulated at the terminals. The system voltages and DSTATCOM voltages must be in phase to achieve proper reactive power flow. The control of this reactive power is attained by a VSC connected across the DSTATCOM and interfaced using a coupling inductor/transformer. The VSC consists of IGBTs and DC source with a self-supporting capacitor. The equivalent circuit of a single-phase STATCOM is shown in Figure 5.2. The operation of the DSTATCOM is as follows: The AC voltage is directly proportional to  $(V_{dc})$  which is the sum of DC voltages  $(V_{dc}/2)$  across the split capacitor as shown in the Figure 5.2. The voltage  $V_{dc}$  is maintained constant by using an energy source such as a battery or a rectifier at DC side. During one cycle,  $T_1$  and  $T_2$  are switched on and off for one time.

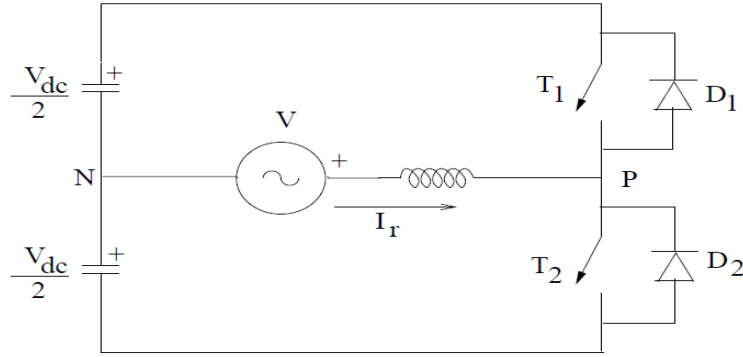
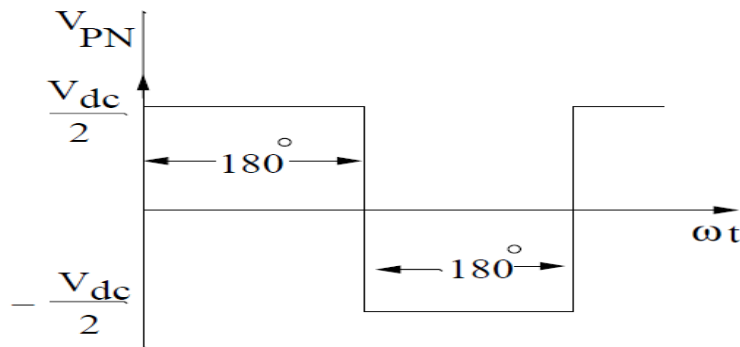


FIGURE 5.2: Equivalent circuit of a single-phase STATCOM

The conduction period of each switch is  $180^\circ$ . It is to be ensured that  $T_1$  is  $0^\circ$  when  $T_2$  is on and vice versa. The diodes D1 and D2 enable the conduction of the current in the reverse direction. The voltage across PN is shown in Figure 5.2.  $V_{PN} = \frac{V_{dc}}{2}$  if  $T_1$  is ON ( $T_2$  is off) and  $V_{PN} =$

FIGURE 5.3: The waveform of  $V_{PN}$ 

$-\frac{V_{dc}}{2}$  if  $T_2$  is ON (and  $T_1$  is off). The switches are operated at frequency  $\omega$  in synchronization with supply voltage. The fundamental RMS component of ( $E_1$ ) is obtained as

$$E_1 = \frac{\sqrt{2}}{\pi} \int_0^\pi \frac{V_{dc}}{2} \sin\theta d\theta = \frac{\sqrt{2}}{\pi} V_{dc} \quad (5.1)$$

A capacitive reactive current is drawn if  $E_1 > V$ , and inductive current is drawn if  $E_1 < V$  by DSTATCOM. The capacitors can be charged accordingly from the source through the diodes. Thus the DC link of the DSTATCOM acts to operate in capacitive or inductive by energizing and de-energizing its DC link accordingly in case of linear loads. However, the performance of DSTATCOM is enhanced by including an appropriate control for mitigation of current harmonics

in case of nonlinear loads. Thus DSTATCOM is modified as shunt APF by adapting filtering feature by using current detecting method as explained in section 4.4.

### 5.3 Classification of Shunt Active Power Filters

Shunt APFs can be classified based on the type of converter used, topology and the number of phases. Based on converter used, the shunt APFs are classified as current source and voltage source (CSC and VSC) APFs. CSC-shunt APF is reliable but lossy and power capacitors with high rating are required. Due to this, can not be applied in case of multilevel mode. Whereas VSC based APF has a self-supporting DC voltage bus. It is preferred due to its lightweight, cheap, and can be extended to multilevel. Based on topology the two types are: Half-bridge, Full bridge and H-bridge shunt APFs. Similarly, based on number of phases the series APF systems are: 1-phase 2-wire, 3-phase 3-wire, and 3-phase 4-wire.

### 5.4 Control Strategy of Shunt APF

The shunt APF is a custom power device that has been designed for mitigating current based problems especially increased neutral currents, harmonic currents along with DC link control. From the literature, the different control algorithms of shunt APF are categorized into time domain (Ex. 3-phase p-q theory) and frequency domain (based on Fourier analysis) [166]. The frequency domain algorithms require heavy computation burden and hence are quite sluggish and slow. Therefore, they are less preferred compared to time-domain control algorithms. Hence the time domain based algorithms are considered in this work. Figure 5.4 gives the overall control of shunt APF. The major functions of the shunt APF are to compensate current harmonics and unbalance currents along with an additional task of maintaining the DC link profile. In this regard, the DC link current and a constant reference current are compared. The reference current is constant and equal in magnitude to the maximum value of current with harmonics. The error is fed to a PI controller which is further added to derivative reference source current of MG is

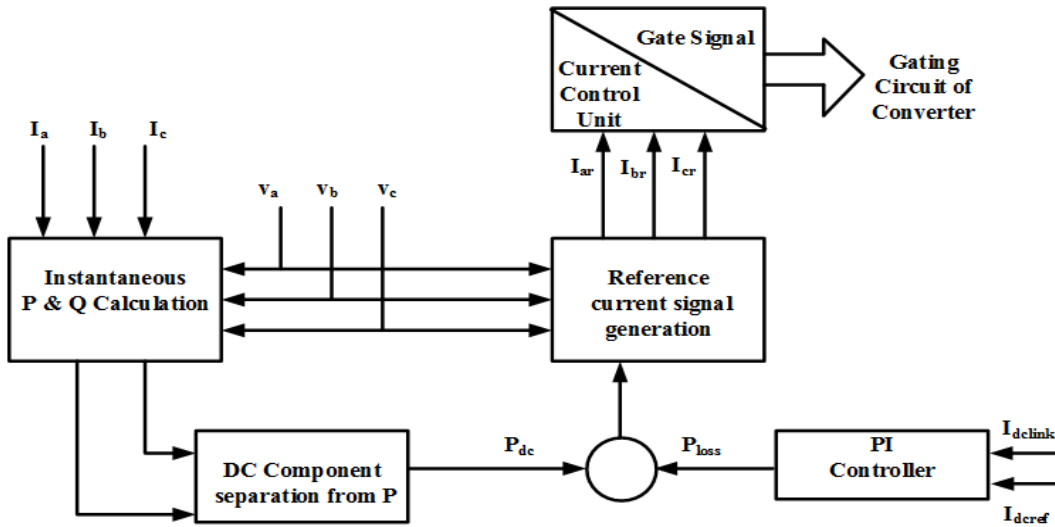


FIGURE 5.4: Control block diagram of Shunt APF controller

shown in Figure 5.5. The modest approach to repay the aforementioned power quality issues can

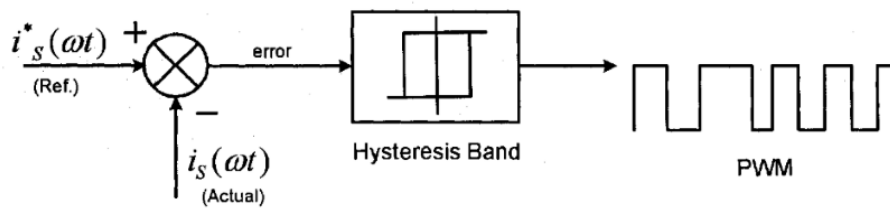


FIGURE 5.5: DC link control

be obtained by making the source current as balanced and sinusoidal. To accomplish this, the DC link voltage is detected and related and the reference DC link voltage, as shown in Figure 5.5. The difference is then fed to a PI controller. The output of the PI controller is maximum of fundamental current,  $I_m$ , which ought to be drawn from the supply  $I_S$  so as to keep up the DC link voltage steady and to supply losses connected with shunt APF. The operation of shunt APF is mainly based on the extraction of reference signals. There are different techniques for generating/extracting reference current signals. Different control techniques that are used to generate the reference current signals are,

- Identity vector template generation (IVTG) technique.
- Instantaneous reactive power (IRPT) theory (or) 3-phase P-Q theory.
- Modified 3-phase P-Q theory (or) proposed single-phase P-Q theory.

### 5.4.1 IVTG control of Shunt APF

The IVTG control algorithm provides simple control at the load terminals (at PCC). This control algorithm of the Shunt APF can be applied for power factor improvement and/or for reactive power compensation. The identity vector template approach mentioned in 4.6.3 for voltages can also be used for currents to generate reference signals for shunt APF. Multiplication of the

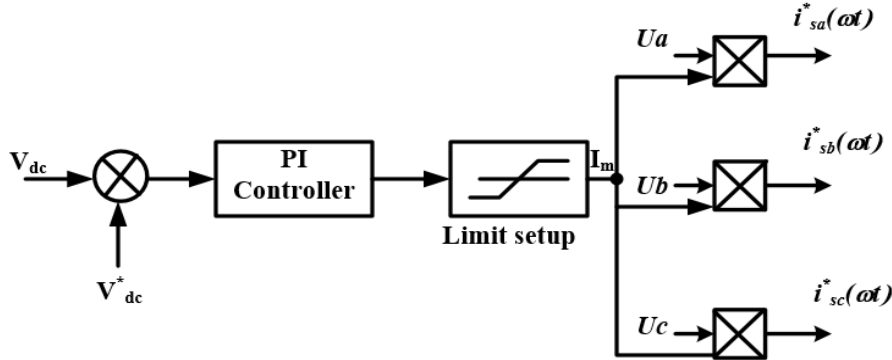


FIGURE 5.6: Shunt APF control using IVTG technique

maximum current  $I_m$  with unit vector layouts derives the balanced, sinusoidal MG source current reference signals as shown in the Figure 5.6.

$$i_{S_a}^*(\omega t) = I_m \cdot U_a = I_m \sin(\omega t) \quad (5.2)$$

$$i_{S_b}^*(\omega t) = I_m \cdot U_b = I_m \sin(\omega t - 120^\circ) \quad (5.3)$$

$$i_{S_c}^*(\omega t) = I_m \cdot U_c = I_m \sin(\omega t - 120^\circ) \quad (5.4)$$

The actual source currents are then compared to these reference signals and is followed by PWM generation achieved by precise switching of inverter to achieve the required parameters. A balance procedure is utilized to produce the sufficient gating signal for PWM generation. A hysteresis procedure is utilized to produce the sufficient gating signal for PWM generation. A hysteresis control is used for PWM generation as shown in Figure 5.5 to control the inverter. The hysteresis controller gives the gating moment at whatever point, the error differs from a preset value as characterized by the hysteresis limits. To control the inverter, the produced reference current signals, for the shunt inverter, are compared with detected source currents individually. At the final, the difference is handled to produce the gating signal configuration for shunt inverters. For



load balancing and to maintain a constant voltage at the PCC shunt APF takes normally a leading current component due to lagging power factor loads as shown in the phasor diagrams Figure 5.7(a) and Figure 5.7(b). Figure 5.7(a) represents the condition of MG without shunt APF. As a result the voltage is dropped to  $V_S$  from  $V_M$  due to impedance  $Z_S$  from parameters  $L_S, R_S$ . A leading current (supply) is drawn when shunt APF is connected that controls the drop across the supply impedance. Hence  $|V_S| = |V_M|$  can be achieved as shown in the Figure 5.7(b). However, this method works well in case of balanced currents. If the neutral currents are increased due to non-linear current harmonic loads, another control is to be considered to compensate the raised neutral currents. Hence, to include the extraction of neutral currents, instantaneous reactive power theory (IRPT) or 3-phase P-Q theory is considered. The following section discusses the 3-phase P-Q theory based control. The advantage of 3-phase P-Q theory is control in terms of active and reactive power components from the considered V, I parameters at the PCC.

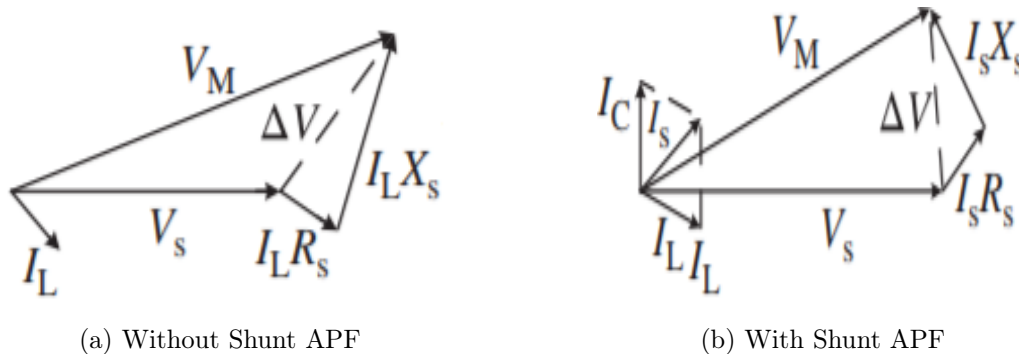


FIGURE 5.7: Phasor diagrams of Shunt APF operation

### 5.4.2 3-phase P-Q Theory

In shunt compensation, the actual source currents are to be compared with the reference current signals and is followed by PWM generation achieved by precise switching of inverter to achieve the required parameters. A balance procedure is utilized to produce the sufficient gating signal for PWM generation. A hysteresis control is used for PWM generation to control the inverter. The hysteresis controller gives the gating moment at whatever point, the error differs from a pre-set value as characterized by the hysteresis limits. To control the inverter, the produced

reference current signals, for the shunt inverter, are compared with detected source currents individually. At the final, the difference is handled to produce the gating signal configuration for shunt inverters. For load balancing and to maintain a constant voltage at the PCC shunt APF takes normally a leading current component due to lagging power factor loads. However, this method works well in case of balanced currents. If the neutral currents are increased due to non-linear current harmonic loads, another control is to be considered to compensate the raised neutral currents. Hence, to include the extraction of neutral currents, instantaneous reactive power theory (IRPT) or 3-phase P-Q theory is considered. The advantage of 3-phase P-Q theory is control in terms of active and reactive power components from the considered V, I parameters at the PCC. Initially, the load currents and MG source voltages are sensed and transformed. In the three phase system the reference signal generation is based on these generalized 3-phase currents and voltages. The block diagram of 3-phase P-Q theory based control algorithm is shown in Figure. 5.8. Initially, the load currents ( $i_{La}, i_{Lb}, i_{Lc}$ ) and MG source voltages ( $V_{sa}, V_{sb}, V_{sc}$ ) are sensed and transformed  $\alpha - \beta$  components ( $V_{\alpha}, V_{\beta}$ ), ( $i_{\alpha}, i_{\beta}$ ) that are given by,

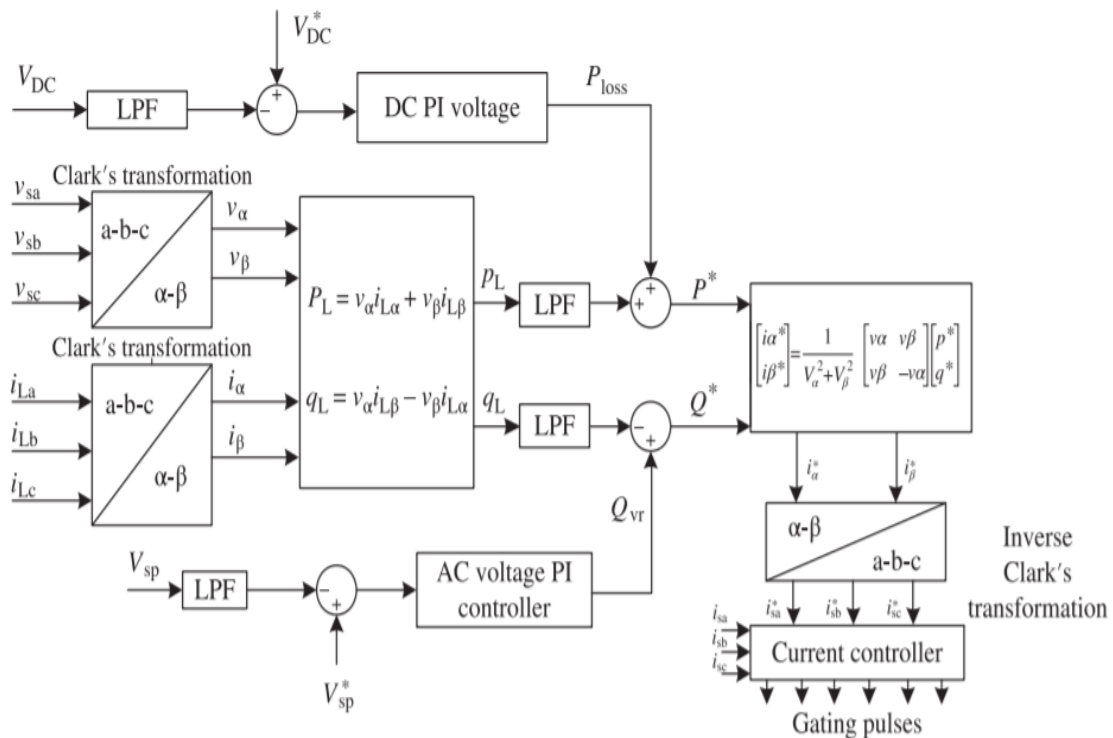


FIGURE 5.8: 3-phase P-Q theory control of Shunt. APF

$$\begin{pmatrix} v_\alpha \\ v_\beta \end{pmatrix} = \sqrt{\frac{2}{3}} \begin{bmatrix} 1 & -\frac{1}{2} & -\frac{1}{2} \\ 0 & -\frac{\sqrt{3}}{2} & \frac{\sqrt{3}}{2} \end{bmatrix} \begin{pmatrix} v_{sa} \\ v_{sb} \\ v_{sc} \end{pmatrix} \quad (5.5)$$

$$\begin{pmatrix} i_\alpha \\ i_\beta \end{pmatrix} = \sqrt{\frac{2}{3}} \begin{bmatrix} 1 & -\frac{1}{2} & -\frac{1}{2} \\ 0 & -\frac{\sqrt{3}}{2} & \frac{\sqrt{3}}{2} \end{bmatrix} \begin{pmatrix} i_{La} \\ i_{Lb} \\ i_{Lc} \end{pmatrix} \quad (5.6)$$

From these, the instantaneous active power  $p_L$  and the instantaneous reactive power  $q_L$  are obtained as

$$\begin{pmatrix} p_L \\ q_L \end{pmatrix} = \begin{pmatrix} v_\alpha & v_\beta \\ v_\beta & -v_\alpha \end{pmatrix} \begin{pmatrix} i_{L\alpha} \\ i_{L\beta} \end{pmatrix} \quad (5.7)$$

Where  $\bar{p}_L$  and  $\tilde{p}_L$  represents the DC, AC components of  $p_L$  respectively. Similarly,  $\bar{q}_L$  and  $\tilde{q}_L$  are the DC, AC components of  $q_L$ . Rewriting the above equations as:

$$p_L = \bar{p}_L + \tilde{p}_L, q_L = \bar{q}_L + \tilde{q}_L \quad (5.8)$$

$\bar{p}_L$  and  $\bar{q}_L$  represent the transformed DC component from fundamental load power,  $\tilde{p}_L$  and  $\tilde{q}_L$  gives the the transformed AC component from the distortion or negative sequence components. A first order LPFs are used to derive the ripple free DC components of p and q. From these, the reference MG supply currents ( $i_{sa}^*, i_{sb}^*, i_{sc}^*$ ) are computed as

$$\begin{pmatrix} i_{sa}^* \\ i_{sb}^* \\ i_{sc}^* \end{pmatrix} = \sqrt{\frac{3}{2}} \begin{pmatrix} 1 & 0 \\ -\frac{1}{2} & \frac{\sqrt{3}}{2} \\ -\frac{1}{2} & -\frac{\sqrt{3}}{2} \end{pmatrix} \begin{pmatrix} v_\alpha & v_\beta \\ -v_\beta & v_\alpha \end{pmatrix}^{-1} \begin{pmatrix} p^* \\ q^* \end{pmatrix} \quad (5.9)$$

From the PI voltage controller over the PCC output voltage,  $p^*$  and  $q^*$  as  $p^* = \bar{p}_L + \tilde{p}_{loss}$  and  $q^* = q_{vr} - \bar{q}_L$  are estimated. The flowchart of 3-phase P-Q theory control is given in Figure 5.9

The 3-phase reference supply currents are deduced, transformed and further compared with sensed supply currents as shown in Figure 5.8 to control shunt APF. The instantaneous active and reactive components in this method consisting DC and oscillating, AC components are computed

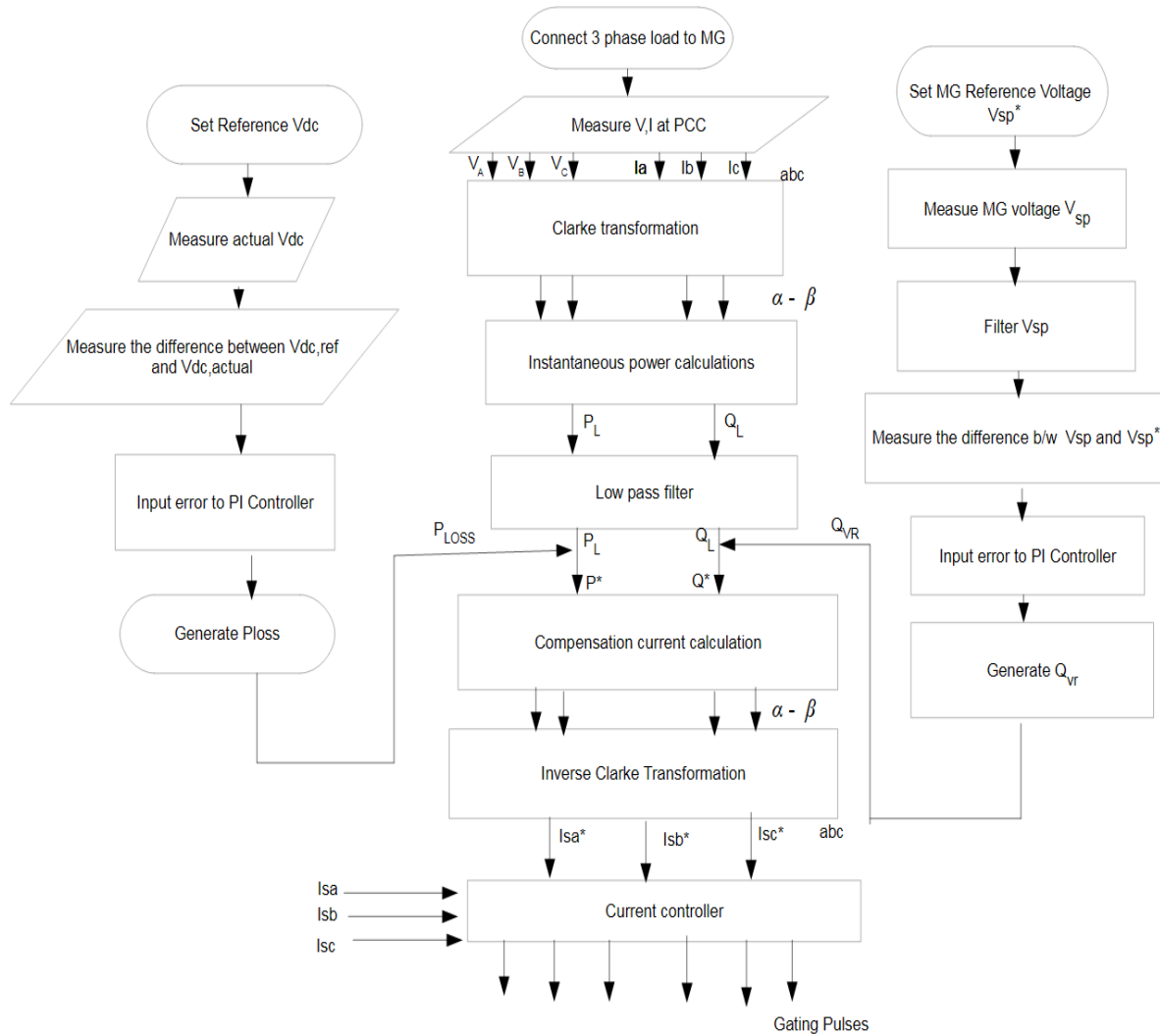


FIGURE 5.9: Flow chart of 3-phase P-Q control of shunt APF

for all the three phases by considering average. Instead of this, it is required to consider the three individual phases consisting average, DC and oscillating, AC components from which the exact average components for all the three phases can be separated. This is more helpful when the MG is delivering an unbalanced and high nonlinear load is connected which distorts the currents in all individual phases very distinctly. Hence, the 3-phase method is further modified as single-phase P-Q theory to extract the individual phase components.

### 5.4.3 Modified 3-Phase P-Q Theory or 1-Phase P-Q Theory

In the three-phase system, the reference signal generation is based on the generalized 3-phase source currents and load voltages. This approach will not produce the suitable reference signals

for the extraction of individual phases which is actually required especially to deal with low voltage level PQ problems. In this regard, the single-phase P-Q control algorithm using time domain control is developed and implemented to control shunt APF. The 3-phase P-Q theory is reframed into a three- single phase systems which can be further represented as a two-phase system with  $90^\circ$  lead or  $90^\circ$  lag in similar to a direct 3-phase system. This results in a two-phase system in which PCC voltages and currents are expressed in terms of  $\alpha - \beta$  coordinates. The representation is continued in the further implementation of the algorithm. By implementing this, the instantaneous active and reactive components of the three individual phases consisting average, DC and oscillating, AC components are computed from which the exact average components for all the three phases can be separated.

#### 5.4.3.1 Current Compensation Approach

In general, the load currents of a 3P4W distribution system are unbalanced due to the unbalance load connected. The system requires compensation in terms of reactive power, to reduce harmonics occurring due to various linear and non-linear loads. To make these currents balanced and to provide required compensation, a novel control strategy is proposed based on modified single-phase p-q theory. This theory states that a single phase system can be a two-phase system with  $90^\circ$  lead or  $90^\circ$  lag. The resultant two-phase system representation is in terms of  $\alpha - \beta$  coordinates with respect to PCC voltages and currents. The control block diagram of the single phase P-Q theory based control algorithm is shown in the Figure 5.10. The load currents ( $i_{La}, i_{Lb}, i_{Lc}$ ), PCC voltages ( $V_{mg,a}, V_{mg,b}, V_{mg,c}$ ), supply currents ( $i_{mg,a}, i_{mg,b}, i_{mg,c}$ ), ( $V_{dc}$ ) of the VSC of the shunt APF represent the actual operating signals of the MG. Load voltages of each phase in terms of  $\alpha - \beta$  coordinates in modified P-Q theory are written as: Phase a-

$$\begin{bmatrix} V_{La,\alpha} \\ V_{La,\beta} \end{bmatrix} = \begin{bmatrix} V_{La}^*(\omega t) \\ V_{La}^*(\omega t + \pi/2) \end{bmatrix} = \begin{bmatrix} V_{Lm} \sin(\omega t) \\ V_{Lm} \cos(\omega t) \end{bmatrix} \quad (5.10)$$

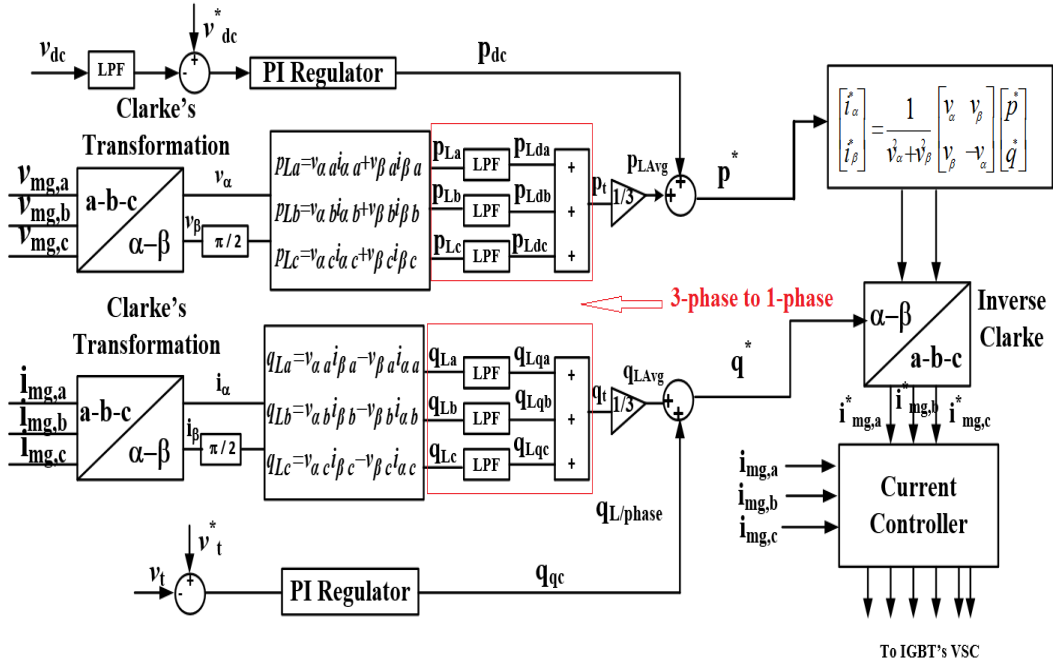


FIGURE 5.10: Single phase P-Q theory control block diagram

$$\begin{bmatrix} i_{La,\alpha} \\ i_{La,\beta} \end{bmatrix} = \begin{bmatrix} i_{La}(\omega t + \phi_L) \\ i_{La}(\omega t + \phi_L) + \pi/2 \end{bmatrix} \quad (5.11)$$

Phase-b

$$\begin{bmatrix} V_{Lb,\alpha} \\ V_{Lb,\beta} \end{bmatrix} = \begin{bmatrix} V_{Lb}^*(\omega t) \\ V_{Lb}^*(\omega t + \pi/2) \end{bmatrix} = \begin{bmatrix} V_{Lm} \sin(\omega t - 120^\circ) \\ V_{Lm} \cos(\omega t - 120^\circ) \end{bmatrix} \quad (5.12)$$

$$\begin{bmatrix} i_{Lb,\alpha} \\ i_{Lb,\beta} \end{bmatrix} = \begin{bmatrix} i_{Lb}(\omega t + \phi_L - 120^\circ) \\ i_{Lb}(\omega t + \phi_L - 120^\circ) + \pi/2 \end{bmatrix} \quad (5.13)$$

Phase-c

$$\begin{bmatrix} V_{Lc,\alpha} \\ V_{Lc,\beta} \end{bmatrix} = \begin{bmatrix} V_{Lc}^*(\omega t) \\ V_{Lc}^*(\omega t + \pi/2) \end{bmatrix} = \begin{bmatrix} V_{Lm} \sin(\omega t + 120^\circ) \\ V_{Lm} \cos(\omega t + 120^\circ) \end{bmatrix} \quad (5.14)$$

$$\begin{bmatrix} i_{Lc,\alpha} \\ i_{Lc,\beta} \end{bmatrix} = \begin{bmatrix} i_{Lc}(\omega t + \phi_L + 120^\circ) \\ i_{Lc}(\omega t + \phi_L + 120^\circ) + \pi/2 \end{bmatrix} \quad (5.15)$$

The instantaneous p and q, using the single-phase approach, can be derived as

$$p_{Lx} = v_{Lx,\alpha} \cdot i_{Lx,\alpha} + v_{Lx,\beta} \cdot i_{Lx,\beta} \quad (5.16)$$

where  $x$  represents a,b,c for three phases.

$$q_{Lx} = v_{Lx,\alpha} \cdot \dot{i}_{Lx,\beta} - v_{Lx,\beta} \cdot \dot{i}_{Lx,\alpha} \quad (5.17)$$

The phase 'a' instantaneous load active and instantaneous load powers can be represented as,

$$\begin{bmatrix} p_{La} \\ q_{La} \end{bmatrix} = \begin{bmatrix} v_{La,\alpha} & v_{La,\beta} \\ -v_{La,\beta} & v_{La,\alpha} \end{bmatrix} \cdot \begin{bmatrix} \dot{i}_{La,\alpha} \\ \dot{i}_{La,\beta} \end{bmatrix} \quad (5.18)$$

Unlike 3-phase P-Q theory, the single-phase P-Q theory considers the instantaneous active powers ( $p_{La}, p_{Lb}, p_{Lc}$ ) of each phase. In turn, these powers include average, DC and oscillating, AC components of each phase. The active powers from average component ( $p_{Lda}, p_{Ldb}, p_{Ldc}$ ) of each phase are extracted and fed to a low pass filter and averaged further as

$$p_{LAvg} = \frac{(p_{Lda} + p_{Ldb} + p_{Ldc})}{3} \quad (5.19)$$

Similarly, the sensed DC bus voltages and the reference DC bus voltage of shunt APF are compared and produce error signal. This error is fed to PI regulator and is represented as  $p_{DC}$  to maintain the DC bus voltage at desired level. The resultant active power component is

$$p^* = p_{LAvg} + p_{DC} \quad (5.20)$$

The terminal voltage  $V_t$  is obtained from  $(v_{mg,a}, v_{mg,b}, v_{mg,c})$  as given by,

$$V_t = \sqrt{\frac{2}{3}(v_{mg,a}^2 + v_{mg,b}^2 + v_{mg,c}^2)} \quad (5.21)$$

Similarly load reactive powers can be obtained as

$$\begin{aligned} q_{La} &= v_{\alpha a} \cdot \dot{i}_{\beta a} - v_{\beta a} \cdot \dot{i}_{\alpha a} \\ q_{Lb} &= v_{\alpha b} \cdot \dot{i}_{\beta b} - v_{\beta b} \cdot \dot{i}_{\alpha b} \\ q_{Lc} &= v_{\alpha c} \cdot \dot{i}_{\beta c} - v_{\beta c} \cdot \dot{i}_{\alpha c} \end{aligned} \quad (5.22)$$

Application of LPF (low pass filter) extracts the average reactive powers from instantaneous values (13) and are indicated as  $q_{La}, q_{Lb}, q_{Lc}$ . The reactive power in balanced single-phase case, with the computed average values, is given by,

$$q_{LAvg} = \frac{(q_{La} + q_{Lb} + q_{Lc})}{3} \quad (5.23)$$

The total reactive power component of the source is represented by,

$$q^* = q_{qc} - q_{LAvg} \quad (5.24)$$

where the component  $q_{qc}$  is due to PI regulator output voltage at PCC. The reference source currents ( $i_{mg,a}^*, i_{mg,b}^*, i_{mg,c}^*$ ) are represented as

$$i_{mg,a}^*(t) = \frac{v_{\alpha a}(t)}{v_{\alpha a}^2 + v_{\beta a}^2} [p_t] + \frac{v_{\beta a}(t)}{v_{\alpha a}^2 + v_{\beta a}^2} [q_t] \quad (5.25)$$

The other phases b,c reference source currents are calculated as

$$i_{mg,b}^*(t) = \frac{v_{\alpha b}(t)}{v_{\alpha b}^2 + v_{\beta b}^2} [p_t] + \frac{v_{\beta b}(t)}{v_{\alpha b}^2 + v_{\beta b}^2} [q_t] \quad (5.26)$$

$$i_{mg,c}^*(t) = \frac{v_{\alpha c}(t)}{v_{\alpha c}^2 + v_{\beta c}^2} [p_t] + \frac{v_{\beta c}(t)}{v_{\alpha c}^2 + v_{\beta c}^2} [q_t] \quad (5.27)$$

These estimated reference source current signals ( $i_{mg,a}^*, i_{mg,b}^*, i_{mg,c}^*$ ) are compared with the measured source current signals ( $i_{mg,a}, i_{mg,b}, i_{mg,c}$ ). The differences are amplified prior fed to a PI current controller. The flowchart of 1-phase P-Q theory control is given in Figure 5.11.

The controller generates the required gating signals for the converter used in shunt APF. Using the gate signals generated the shunt APF compensates the reactive and harmonic components flowing in the system by injecting required compensation current obtained from the converter.



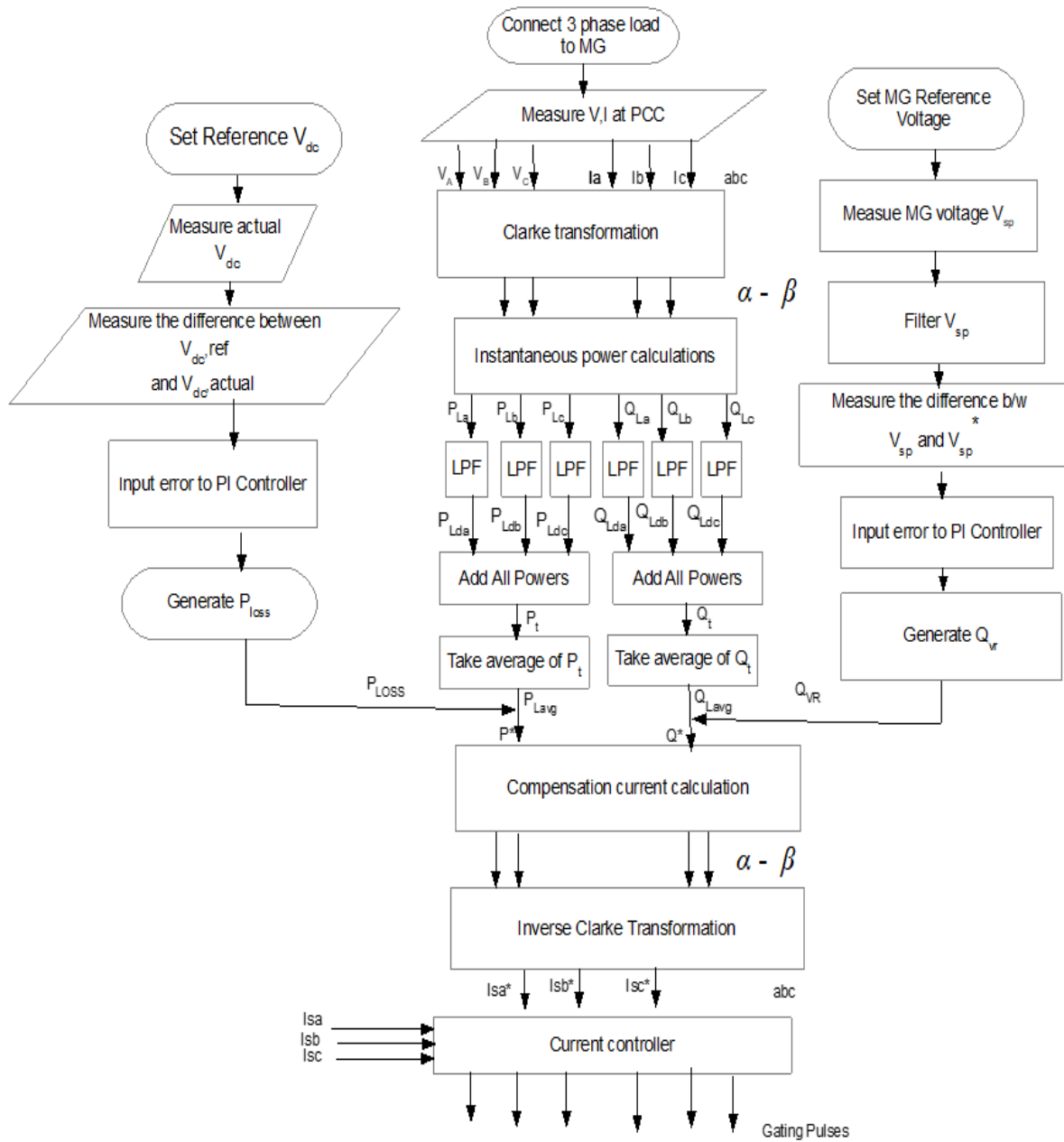


FIGURE 5.11: Flow chart of 1-phase P-Q control of shunt APF

### 5.4.3.2 Neutral Current Compensation

The computed balanced source currents from the unbalanced load currents will be generated using current unbalance approach. The actual neutral current can be calculated by summing all load currents and is given by

$$i_{L,N}(t) = i_{La}(t) + i_{Lb}(t) + i_{Lc}(t) \tag{5.28}$$

The reference neutral current can be given as,

$$i_{Sh,N}^*(t) = -i_{L,N}(t) \quad (5.29)$$

By generating the reference neutral current, shunt APF provides neutral current compensation of 3- phase 4- wire distribution microgrids.

## 5.5 Design of Shunt APF for Power Quality Compensation

The MG is connected to a nonlinear load with diode bridge converter drawing 60 A constant DC current. This high non linear load creates harmonics with 150.84% THD in source current. To mitigate these harmonics a shunt APF has been designed based on the following conditions. The switching frequency is considered as 20 kHz. It is assumed that the DC bus voltage control limit is 8% range and inductor ripple current limit is 5%. The supply voltage i.e. MG output voltage distortion at PCC is negligible. With these conditions applied, the design of shunt APF is as follows:

The MG output RMS phase-a voltage with frequency 50 Hz is  $V_{Mg,a} = 415/\sqrt{3}$ ,  $V_{LL} = 415V$

The load current due to non linear diode bridge converter =  $I_{DC}$ .

The DC bus voltage across the capacitor is given by

$$V_{DC,APF} = \frac{2\sqrt{2}V_{Mg,a}}{m_a} \quad (5.30)$$

where  $m_a$  is modulation index = 0.9. The minimum DC bus voltage required across the capacitor (split capacitor topology for LV applications) is given by

$$V_{DC,min} = \frac{\sqrt{3} * \sqrt{2}}{0.87} * V_{Mg,a} \quad (5.31)$$

The interfacing inductance of the shunt APF is

$$L_{f,interface} = \frac{\sqrt{3}m_a V_{DC,APF}}{2 * 6 * a f_s * \Delta I_f} \quad (5.32)$$

where  $a$  is overload factor =1.2.

$$C_{DC} = \frac{2\Delta E}{(V_{DC,APF}^2 - V_{DC,minAPF}^2)} = \frac{3V_f I_f \Delta t}{(V_{DC,APF}^2 - V_{DC,minAPF}^2)} \quad (5.33)$$

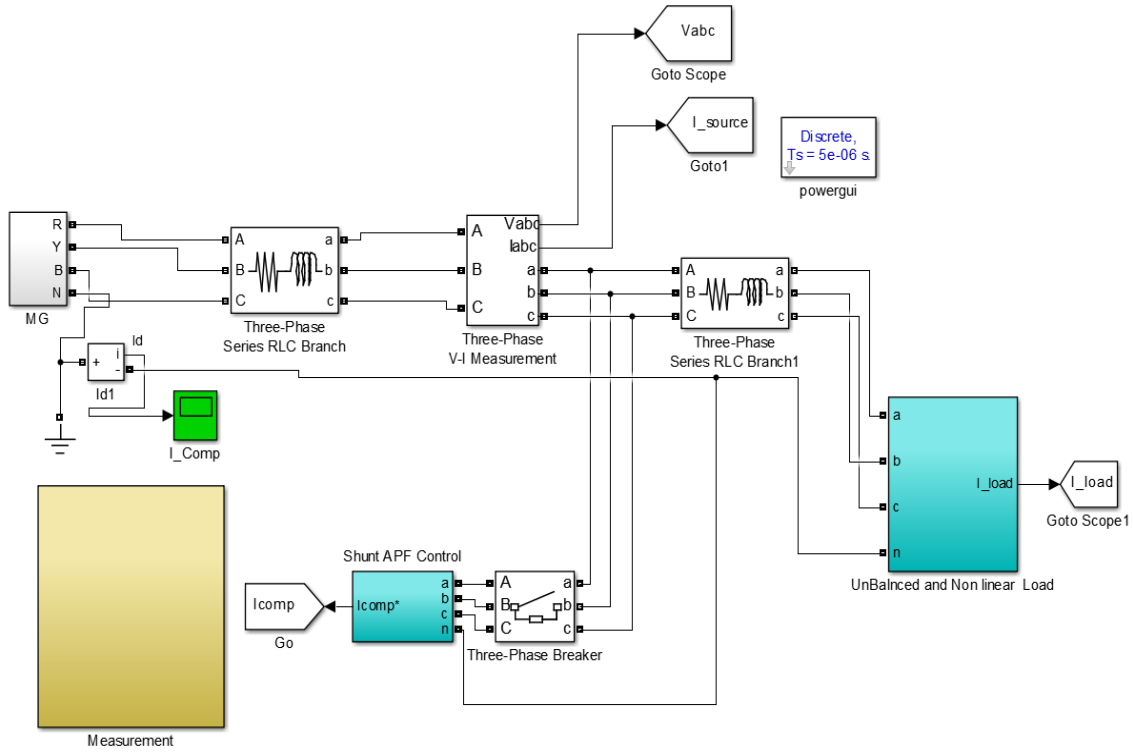


FIGURE 5.12: Simulink diagram of unbalance and neutral compensation using Shunt APF in MG

TABLE 5.1: Design parameters of Shunt APF

Electrical Parameters	Value in Units
Microgrid Reference Voltage $V_s$ or $V_{MG}$	415V
Fundamental Frequency $f$	50Hz
Source Inductance $L_s$	0.5 mH
Ref. DC bus voltage $V_{DC}$	680V
DC bus capacitor $C_{DC}$	2000 $\mu$ F
Inverter Coupling $L_{Sh}$	5.583mH

Using above design procedure, the shunt APF parameters are computed and given in Table. 5.1. Two different non-linear loads that give unbalance and high harmonics in load currents are connected to the MG are listed in Table. 5.2 and Table. 5.3 Based on the filter and DC

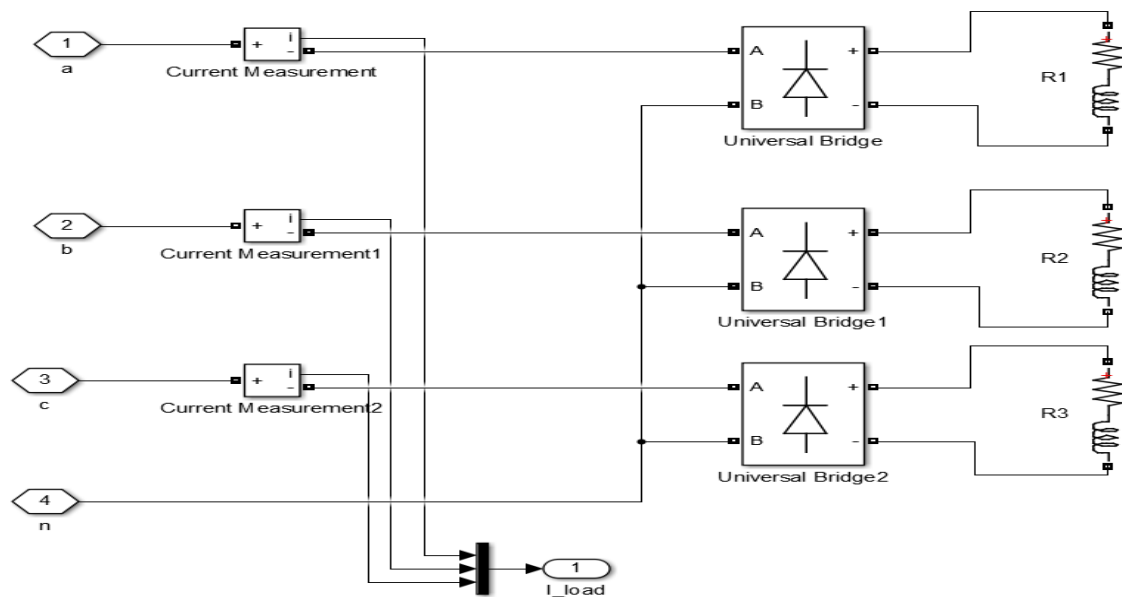


FIGURE 5.13: Unbalance loads connected in MG

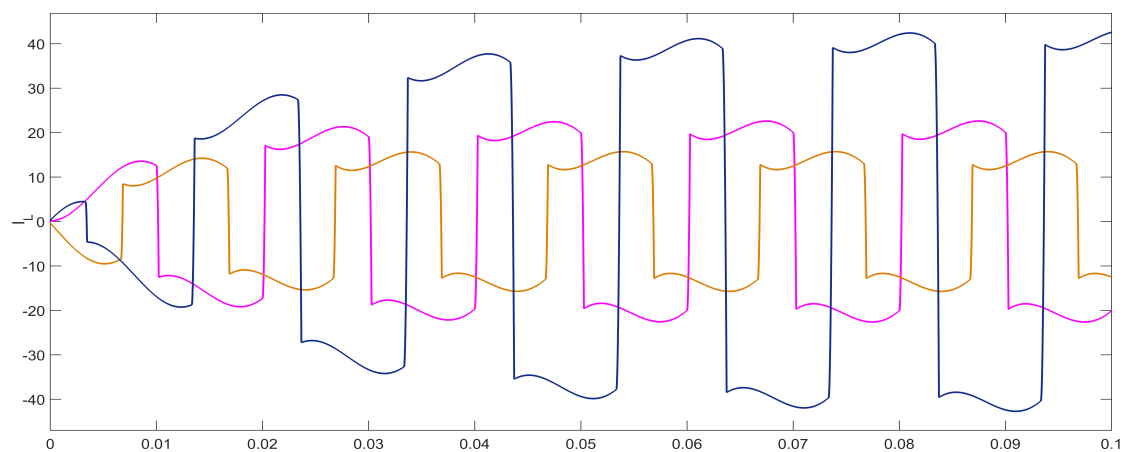


FIGURE 5.14: Unbalance currents due to unbalance loads connected in MG

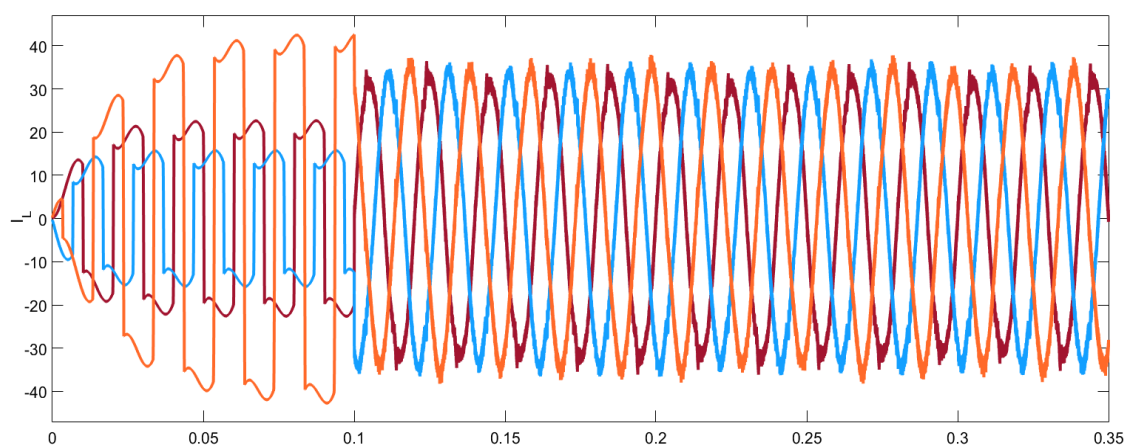


FIGURE 5.15: Unbalance current compensation using Shunt APF in MG

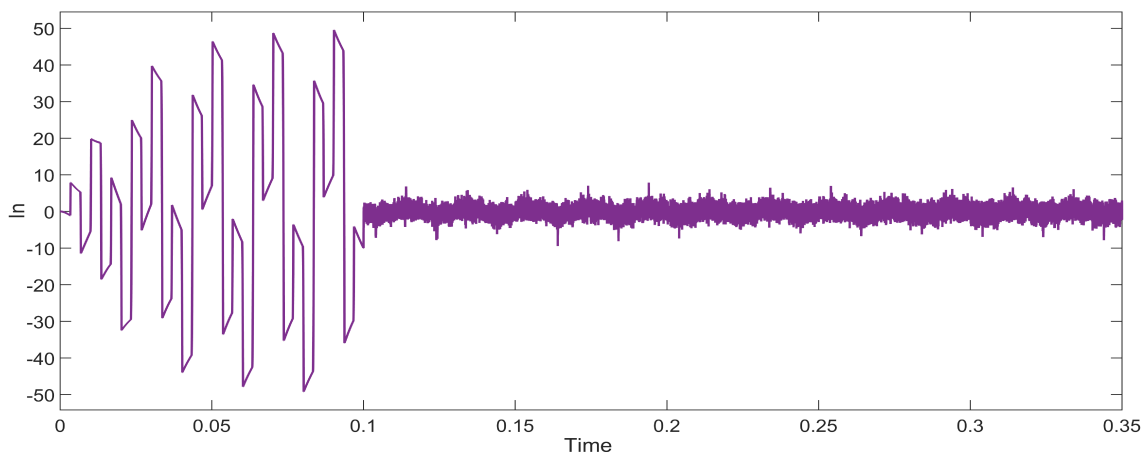


FIGURE 5.16: Neutral current compensation using Shunt APF in MG

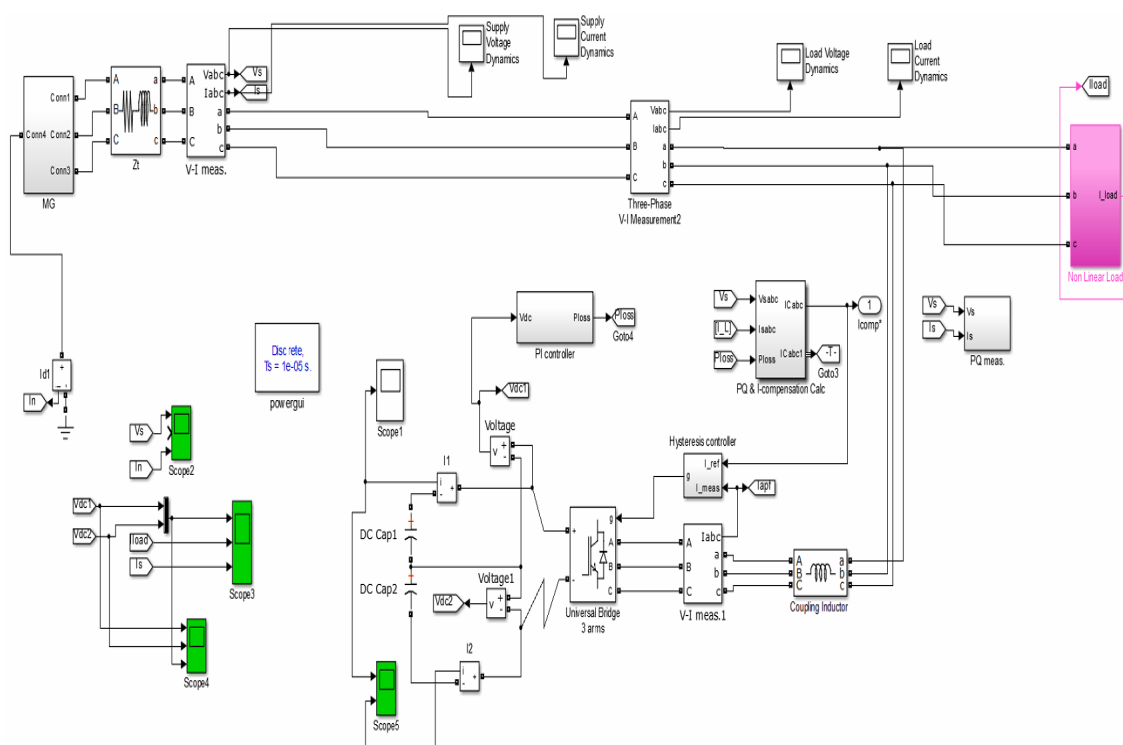


FIGURE 5.17: Simulink diagram of Shunt APF, Single phase P-Q theory control in MG

TABLE 5.2: Details of connected unbalanced nonlinear load

Load (Y-connected)	Value
Load 'a'	Series RL impedance of $30 + j22 \Omega$
Load 'b'	Series RL impedance of $60 + j31.4 \Omega$
Load 'c'	Series RL impedance of $120 + j125.6 \Omega$
Source impedance ( $Z_t$ )	series RL impedance of $0.01 \Omega + j0.002 \text{ mH}$
Nonlinear load	series RL impedance of $0.1 \Omega + j0.4 \text{ mH}$ along with half controlled diode converter

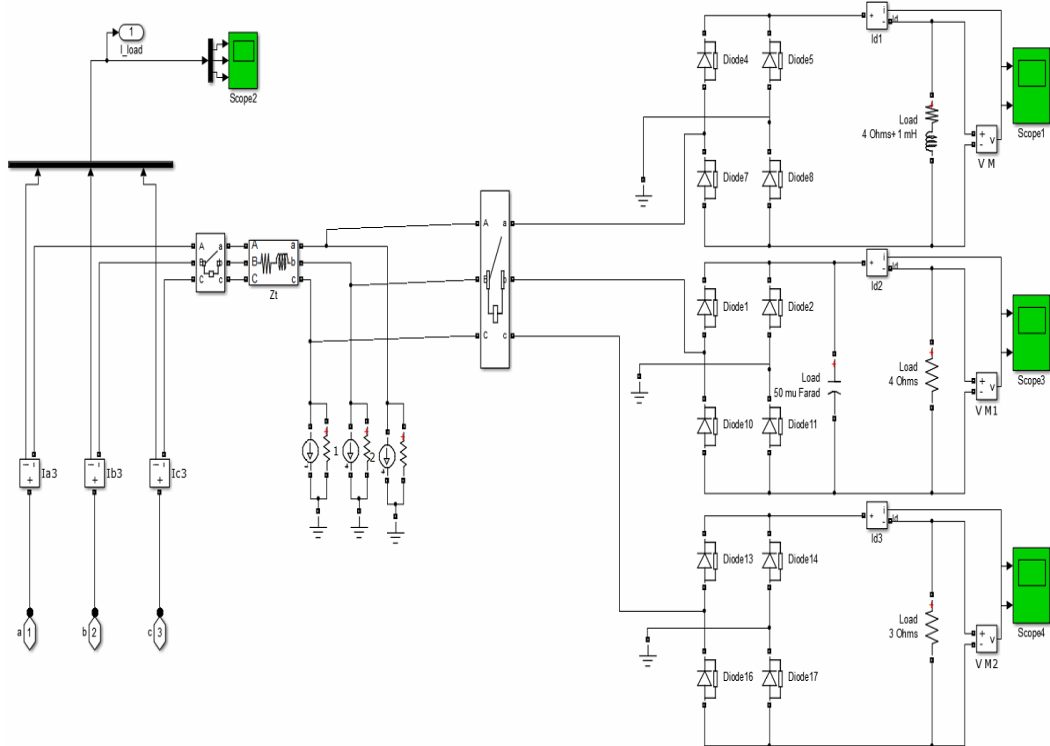


FIGURE 5.18: Non-linear harmonic load connected in MG

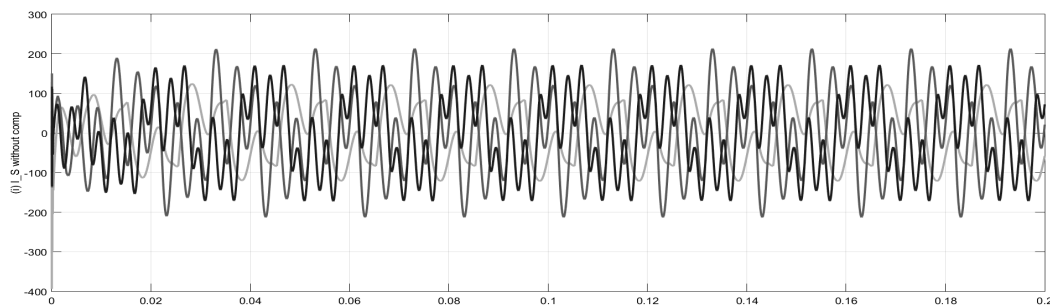


FIGURE 5.19: Source current with harmonics

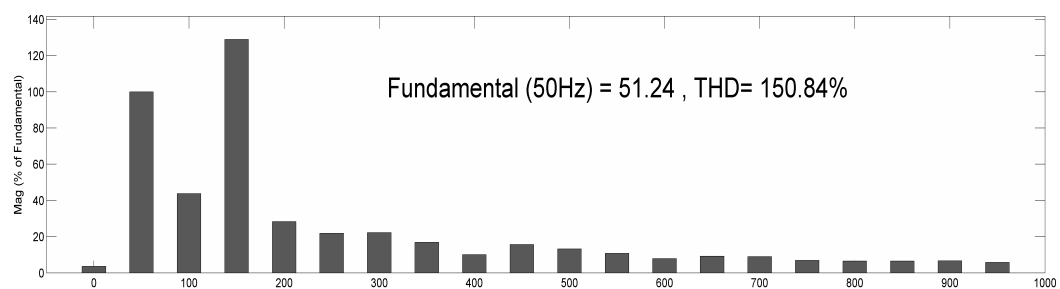


FIGURE 5.20: Source current with harmonics and without Shunt APF

TABLE 5.3: Details of connected loads

Load (Y-connected)	Value
Load 'a'	1-phase diode FBR with series RL load of $4 \Omega + j1 \text{ mH}$
Load 'b'	1-phase diode FBR with parallel RC load of $4 \Omega + j 50 \mu\text{F}$
Load 'c'	1-phase diode FBR with series R load of $3 \Omega$
Source impedance ( $Z_t$ )	series RL impedance of $0.01 \text{ m}\Omega + j 0.1 \text{ mH}$

link parameters computed, shunt APF has been designed and the following section discusses the implementation of shunt APF into MG.

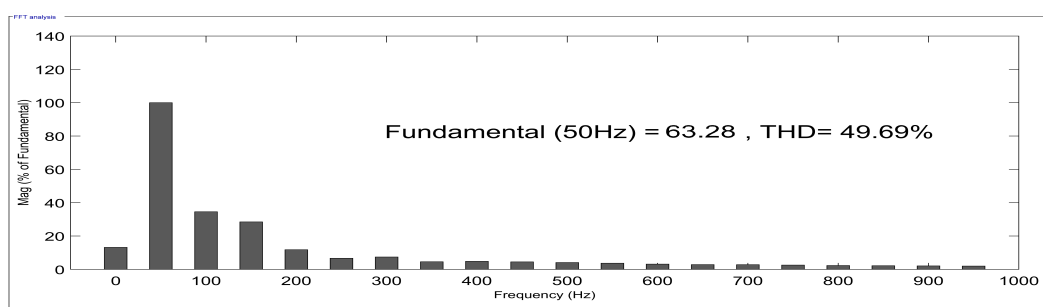


FIGURE 5.21: Source current with harmonics compensated using 3-phase P-Q theory controlled Shunt APF

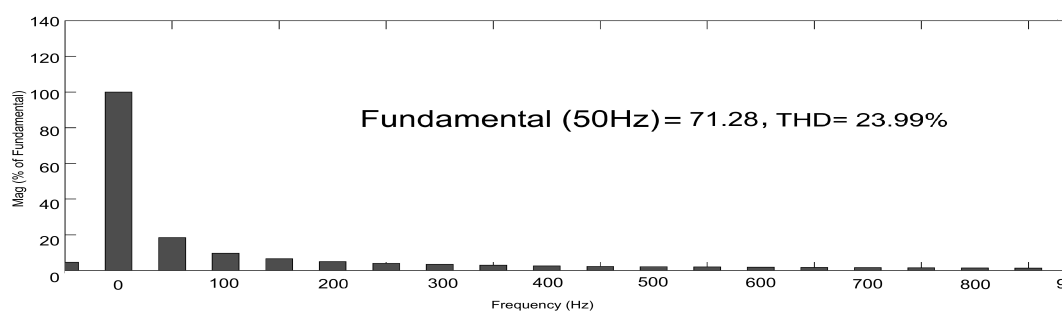


FIGURE 5.22: Source current with harmonics compensated using modified P-Q theory controlled Shunt APF

## 5.6 Simulation of Shunt APF in MG for Current Compensation

The microgrid model is developed with 2 DERS, a PV generator of 1.5 kW and a wind generator 2 kW along with storage to deliver an output voltage of 3-phase, 415 V, 50 Hz, phase to ground voltage of 338 V which is at common AC bus in MATLAB Simulink as discussed in the chapter. 2 and chapter. 4. To this MG, an unbalanced nonlinear load mentioned in Table. 5.2 is connected.

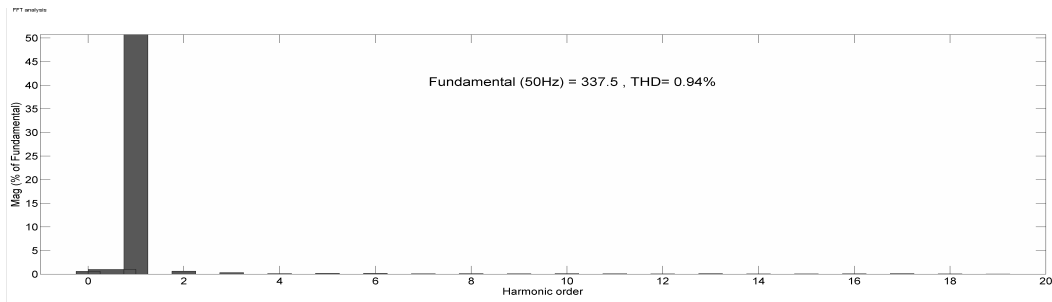


FIGURE 5.23: Load voltage profile during shunt compensation

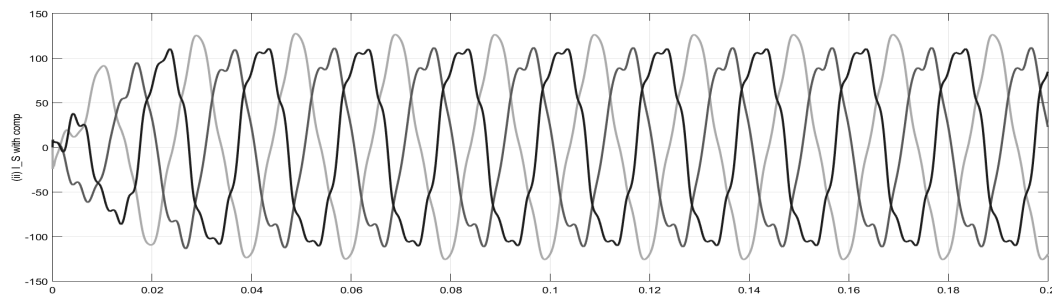


FIGURE 5.24: Source current with harmonics compensated using 1-phase P-Q theory controlled Shunt APF

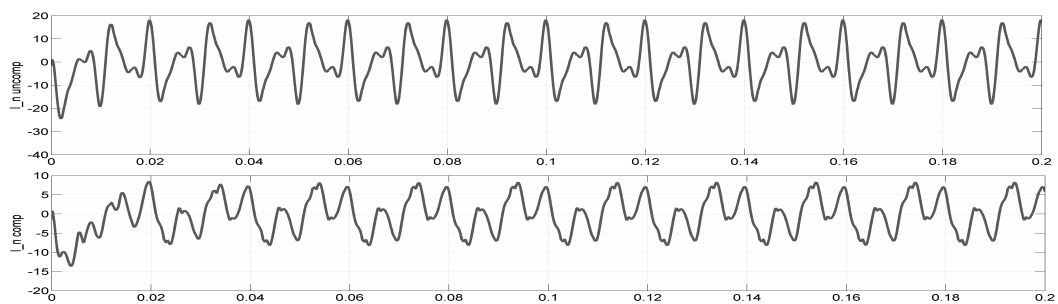


FIGURE 5.25: Neutral current compensation with and without Shunt APF

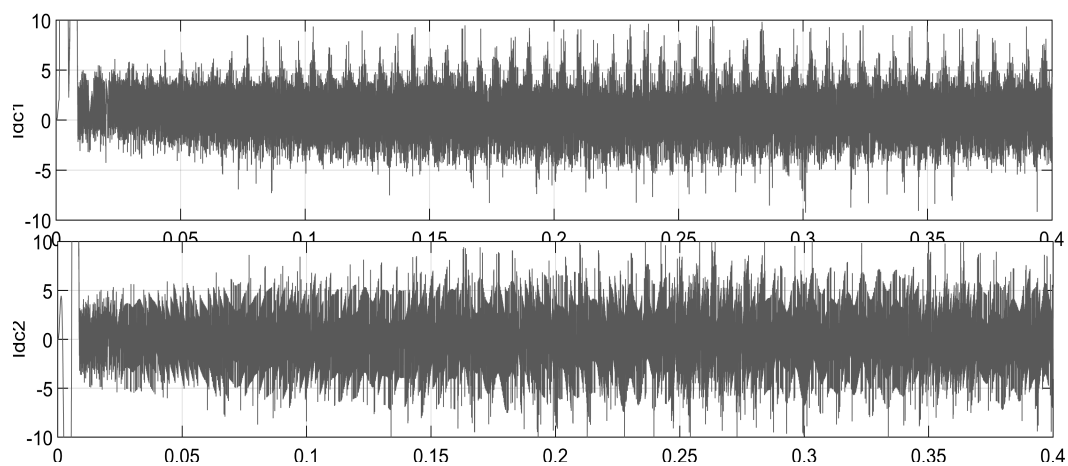


FIGURE 5.26: DC link current profiles of split capacitor based Shunt APF



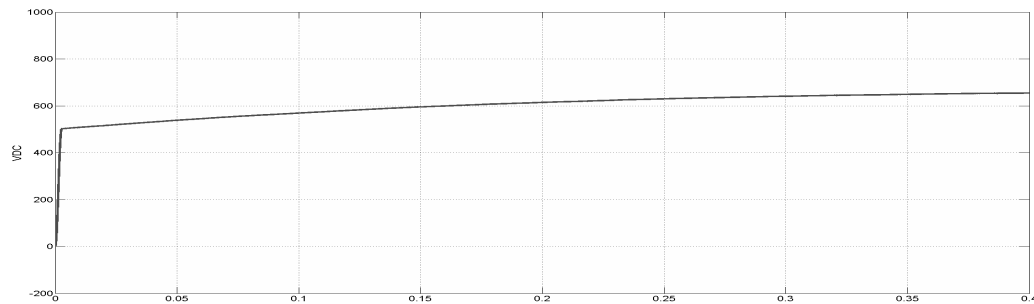


FIGURE 5.27: DC link voltage profile of Shunt APF

The Simulink diagram is shown in Figure 5.12.

The unbalanced load mentioned in Table. 5.2 with different loads in three phases is connected to the MG along with a nonlinear load. As a resultant load current becomes unbalanced which in turn flow towards PCC and source. Hence the currents at source and PCC become unbalanced. To provide compensation for this unbalanced load current, DSTATCOM is used with the above-mentioned control techniques. The DSTATCOM is developed and connected to the system at PCC and just before the load as shown in Figure 5.12 at 0.1 sec. The unbalanced loads connected in MG is shown in Figure 5.13. The load current  $I_L$  containing unbalanced currents is shown in Figure 5.14. The unbalance in the currents is compensated from 0.1 sec as DSTATCOM is connected at 0.1 sec as shown in the Figure 5.15. Similarly, the neutral current compensation from 0.1 sec by using DSTATCOM is shown in Figure 5.16.

The Simulink diagram of Shunt APF in MG with self-controlled DC link (with split capacitor topology for LV applications) with the P-Q theory control is as shown in Figure 5.17. To evaluate the performance of DSTATCOM for current harmonics, another nonlinear load mentioned in Table. 5.2 that gives high current harmonics is connected to the MG as shown in Figure 5.18. When the aforementioned nonlinear load is connected, the response of source current is shown in Figure 5.19 which is harmonic in nature. The THD analysis of source current responses indicates a harmonic component of 150.84% without APF as shown Figure 5.20.

When Shunt APF is applied with 3-phase P-Q theory, the % THD is improved to 49.69% as shown in the Figure 5.21. When Shunt APF is applied with modified 1-phase P-Q theory, the source current harmonics are compensated further and the % THD improvement is also increased to 23.99% as shown in the Figure 5.22. The source current with compensation is shown in Figure

TABLE 5.4: % THDs comparison for shunt compensation

S.No	%THD
Actual	150.84
3-phase P-Q Theory	49.69
1-phase P-Q Theory	23.99

5.24. Correspondingly, the load voltage has a THD of 0.94 % given in Figure 5.23.

The % THDs in all three cases are listed in the Table. 5.4. Similarly the flow of circulating neutral currents in the system due to this non-linear load without Shunt APF is shown in the Figure 5.25. However, the circulating currents are minimized by using Shunt APF during shunt compensation is also shown in Figure 5.25.

The DC link profile of the Shunt APF in MG during power quality compensation is also analyzed. As mentioned in 5.5, split capacitor topology based DC control is used for Shunt APF as shown in the Figure 5.17. The corresponding DC link currents ( $I_{DC1}$ ,  $I_{DC1}$ ) and DC link voltage variations during the operation of Shunt APF are shown in 5.26, 5.27 respectively. Hence the effectiveness of the shunt APF in providing source current harmonic and neutral current compensation is verified.

## 5.7 Conclusion

Power quality issues in terms of current that are resulted from supply and load changes mentioned in 3.5, a shunt APF is applied to provide compensation for current quality problems. In this regard, current harmonics and flow of circulating currents problems in MG for different nonlinear load conditions are observed and presented. The DSTATCOMs are mainly used for providing current quality compensation for these current based power quality problems. Initially, the Shunt APF is employed with IVTG and 3-phase P-Q theory controls to provide harmonic compensation is observed. Due to the sensitivity of MG for individual phase problems at a lower level, the 3-phase theory has been modified to single-phase P-Q theory. The proposed single-phase P-Q theory performance is observed in terms of the improvement in % THD and is presented. The

simulation shows that the Shunt APF effectively provides harmonic and neutral compensation thus the performance is satisfactory with DC link control that acts to the load changes accordingly.